Journal of Medicinal Chemistry

Article

In Vitro and In Vivo Demonstration of Human Ovarian Cancer Necrosis through a Water Soluble and Near Infrared Absorbing Chlorin

Betsy Marydasan, Bollapalli Madhuri, Shirisha Cherukommu, Jedy Jose, Mambattakkara Viji, Suneesh C Karunakaran, Tavarekere K. Chandrashekar, Kunchala Sridhar Rao, Ch. Mohan Rao, and Danaboyina Ramaiah

J. Med. Chem., **Just Accepted Manuscript** • DOI: 10.1021/acs.jmedchem.8b00460 • Publication Date (Web): 16 May 2018

Just Accepted

ACS Publications

is published by the American Chemical Society. 1155 Sixteenth Street N.W., Washington, DC 20036

In Vitro and *In Vivo* Demonstration of Human Ovarian Cancer Necrosis through a Water Soluble and Near Infrared Absorbing Chlorin

Betsy Marydasan,[†] Bollapalli Madhuri,[‡] Shirisha Cherukommu,[‡] Jedy Jose,[‡] Mambattakkara Viji,[†] Suneesh C. Karunakaran,[†] Tavarekere K. Chandrashekar,[§] Kunchala Sridhar Rao,*[,#] Ch. Mohan Rao,*[,‡] and Danaboyina Ramaiah*[,∥]

†Chemical Sciences and Technology Division, CSIR-National Institute for Interdisciplinary Science and Technology (CSIR-NIIST), Trivandrum - 695 019, India

‡CSIR-Centre for Cellular and Molecular Biology (CSIR-CCMB), Hyderabad - 500 007, India

§National Institute of Science Education and Research (NISER), Bhubaneswar - 751 005, India

∥CSIR-North East Institute of Science and Technology (CSIR-NEIST), Jorhat - 785 006, India

Indo-American Cancer Research Foundation (IACRF), Basavatarakam Indo-American Cancer Hospital and Research Institute, Hyderabad 500034

* Corresponding authors:

E-mail: rama@neist.res.in., Tel: +91 3762370012; Fax: +91 3762370011

E-mail: research.director@induscancer.com., Telefax: 91-40-23540348

E-mail: mohan@ccmb.res.in., Tel: 91-40-27195630; Fax: 91-40-27195633

Keywords: Dihydroxychlorin; Singlet oxygen; Photodynamic therapy; Ovarian cancer; Necrosis

ABSTRACT

With an objective to develop efficient sensitizers for therapeutical applications, we synthesized a water soluble, 5,10,15,20-tetrakis(3,4-dihydroxyphenyl)chlorin (**TDC**), and investigated its *in vitro* and *in vivo* biological efficacy and compared with the commercially available sensitizers. **TDC** showed high water solubility (6-fold), when compared to Foscan and exhibited excellent triplet excited state (84%) and singlet oxygen (80%) yields. *In vitro* photobiological investigations in human ovarian cancer cell lines SKOV-3 showed high photocytotoxicity, negligible dark toxicity, rapid cellular uptake and specific localization of **TDC** in neoplastic cells as assessed by flow cytometric cell-cycle and propidium iodide staining analysis. The photodynamic effects of **TDC** have confirmed the reactive oxygen species induced mitochondrial damage leading to necrosis in SKOV-3 cell lines. The *in vivo* photodynamic activity in nude mice models demonstrated abrogation of tumor growth without any detectable pathology in skin, liver, spleen, kidney, thereby **TDC** application as an efficient and safe photosensitizer.

INTRODUCTION

Photodynamic therapy (PDT) is a new approach for a safe and effective eradication of different types of cancerous tissues without affecting the normal cells. This emerging technique is based on the light activation of the sensitizer and the production of reactive oxygen species (ROS) in presence of molecular oxygen.[1-5] PDT induces oxidative damage and can trigger either necrosis or apoptosis mediated cell death depending on the intensity of the insult.[6-9] The reactive oxygen species can also prevent tumor growth indirectly through vascular shutdown and activation of immune response.[4,5,10-17] In this modality, the sensitizer plays a key role in

determining the efficacy of the photodynamic therapy. A series of sensitizers such as porphyrins, porphycenes, phthalocyanines, chlorins, bacteriochlorins, squaraines, rose bengal, methylene blue, and their derivatives, which exhibit good singlet oxygen generation efficiency have been evaluated for the photodynamic treatment.[18-24] Among these, the first generation sensitizer, hematoporphyrin derivative (HpD), which is commercially known as Photofrin@ is being in clinical use for the treatment of several types of cancers.[25] However, HpD has disadvantages like it is a mixture of nine components, has relatively weak absorption at 630 nm and is known to cause skin photosensitivity.[26,27]

In the last few decades, the major challenge in the field of photodynamic therapy has been to overcome the drawbacks of HpD and to discover second generation photosensitizers by red shifting the absorption of Q bands together with high extinction coefficients in the red region. In this effort, several compounds have been investigated for anti-cancer PDT activity.[28] Among these, 5,10,15,20-tetra(m-hydroxyphenyl)chlorin, commercially known as Foscan, is one of the promising sensitizer, which is a reduced form of the porphyrin.[29] But the main disadvantages associated with Foscan are its poor solubility in aqueous media and its high photosensitivity to the patients even up to twenty days after PDT treatment.[30] The porphyrin based photosensitizers developed so far are either heterogeneous in their chemical composition, water insolubility, and have less photodynamic efficiencies or associated with extended cutaneous sensitivity.[31-33] The second generation chlorin derived photosensitizers are chemically pure, but are minimally soluble in aqueous medium.[33,34] Several attempts are being made to overcome these drawbacks by functionalizing the photosensitizers by attaching folic acid, lipid encapsulation etc.[35] However, these additional methodologies compromise on the targeting, toxicity and shelf life. Both Photofrin and Foscan that are approved for clinical use have extended photosensitivity or

required prolonged treatment of light exposure for periods ranging for up to one week. Herein, we report a novel water soluble sensitizer, 5,10,15,20-tetrakis(3,4-dihydroxyphenyl)chlorin (**TDC**) and investigation of its photophysical and *in vitro* and *in vivo* photobiological aspects as compared to Photofrin and Foscan. Uniquely, **TDC** exhibited high absorption and photodynamic activity in human ovarian cancer cells-SKOV-3 and acted as anti-tumor agent *in vivo*, using nude mice models, thereby demonstrating its use as an effective sensitizer in PDT applications.

RESULTS AND DISCUSSION

Synthesis and Photophysical Properties. The synthesis of the 3,4-dimethoxyporphyrin was achieved through the modified procedure of Lindsey method,[36] while the chlorin derivative, **TDC** was accomplished by the reduction of the corresponding porphyrin as shown in Scheme 1. The starting materials and chlorin derivatives were purified through column chromatography as well as through recrystallization and were characterized on the basis of various analytical and spectral evidences. **TDC** showed the characteristic chlorin absorption having a Soret band at 421 nm, and four Q-bands at 521, 550, 596 and 650 nm. When compared to the porphyrins, the Q-band at 650 nm in **TDC** was found to be relatively intense and exhibited an extinction coefficient value of 1.5 x 10^4 $M^{-1}cm^{-1}$. The emission spectrum of dihydroxychlorin **TDC** exhibited two maxima at 654 and 722 nm with a fluorescence quantum yield (Φ_F) of 0.01 ± 0.002 in methanol (Figure 1A).

Scheme 1. Synthesis of the chlorin derivative TDC.

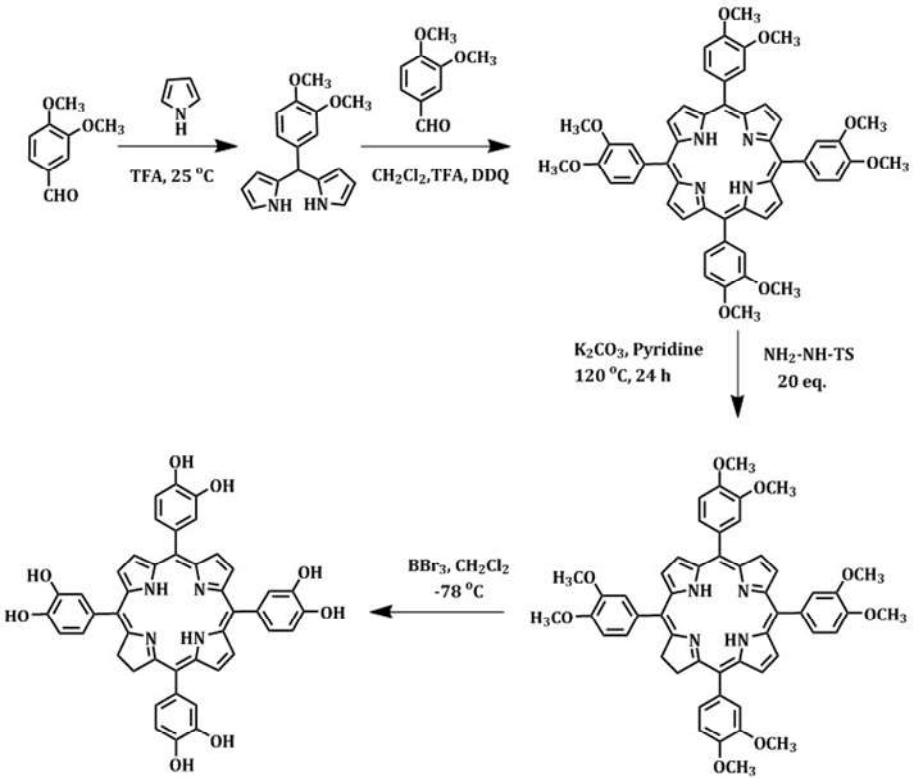

TDC

To understand the transient intermediates involved in the case of the chlorin derivative **TDC**, we have carried out the nanosecond laser flash photolysis experiments. As the first step of this investigation, we have monitored the transient absorption spectrum of **TDC** in DMSO immediately after 355 nm laser pulse excitation. The transient absorption of **TDC** showed an absorption maximum at 360 nm with bleach at 420 nm and the transient intermediate formed from **TDC** decayed by a first-order process with a lifetime of 60 μs. Further, we quantified the triplet quantum yield of (Φ_T) **TDC** employing triplet-triplet energy transfer method and using β-carotene as the energy acceptor.[37] We obtained a triplet quantum yield value of *ca.* $\Phi_T = 0.84 \pm$

0.02 (Figure 1B) for **TDC**, which is better than the values reported for Photofrin and Foscan (Table 1) under similar conditions.

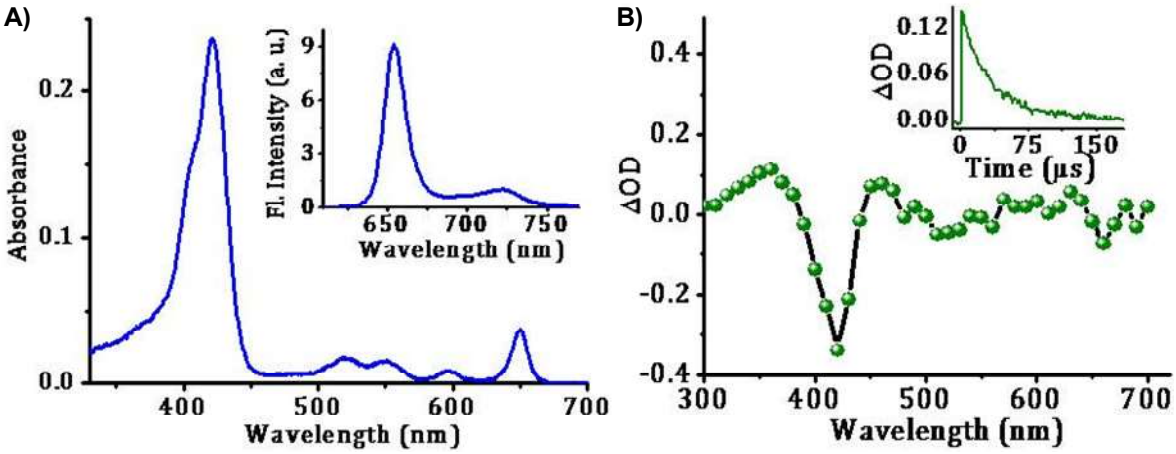

Figure 1. A) UV-Vis absorption and fluorescence (inset) spectra of **TDC** (6 μM) in methanol; λ_{ex}, 430 nm and B) transient absorption spectra of **TDC** (30 μM) following 355 nm laser pulse excitation; time-resolved absorption spectra recorded at 10 μs. The inset shows the transient decay of **TDC** at 440 nm.

To have a better understanding of the PDT efficacy of **TDC**, we have determined the singlet oxygen generation efficiency using chemical trapping method using 1,3-diphenylisobenzofuran (DPBF) as the singlet oxygen scavenger[38] as well as by quantification of its emission intensity at 1270 nm.[39] To determine the singlet oxygen quantum yields [Φ ($^1O_2$)], irradiation of a solution containing the chlorin system **TDC** along with DPBF was carried out using a 200 W mercury lamp as light source with a 515 nm long pass filter at 0-60 s time intervals (Figure S1, Supporting Information). The singlet oxygen generation efficiency [Φ ($^1O_2$)] of **TDC** was found to be *ca.* 0.80 ± 0.03. Interestingly, a comparative study showed higher singlet oxygen generation efficiency for **TDC** in comparison with commercially available

sensitizers, Photofrin and Foscan (Table 1). Moreover, the hydrophilicity of **TDC** due to the presence of hydroxyl groups imparts better solubility for the compound in biological media (Table S1, Supporting Information). For example, the compound **TDC** exhibited *ca.* 6-fold enhancement (3.64 mM) in solubility in 25% aqueous ethanolic medium, when compared to the commercially available sensitizer, Foscan (0.6 mM). In addition to that, the increased solubility decreases the aggregation in aqueous medium, enhances its cellular uptake and bioavailability, aiding in faster plasma clearance and thereby contributing to the higher photodynamic efficacy of **TDC**, when compared to Photofrin and Foscan under similar conditions.[40]

Table 1. Quantum yields of triplet (Φ_T) and singlet oxygen [Φ ($^1O_2$)] yields of sensitizers.[a]

Sensitizer	$\lambda_{ab,}$ nm (ε, $M^{-1}cm^{-1}$)	Φ_F	Φ_T	$\Phi(^1O_2)$
Photofrin	628 (3.0 x 10^3)	0.10	0.60	0.30
Foscan	651 (1.3 x 10^4)	0.08	0.80	0.59
TDC	650 (1.5 x 10^4)	0.01	0.84	0.80

[a] Average of more than three independent experiments. The quantum yields of fluorescence, triplet excited states and singlet oxygen was determined under similar experimental conditions. The values obtained for Photofrin and Foscan are similar to those reported in the literature.[25,33]

Investigation of *In Vitro* Photocytotoxicity. To investigate the photobiological effects of **TDC**, we selected human ovarian cancer cell lines SKOV-3 and a tunable light source-Waldman PDT 1200L (Germany), with an emission spectrum in the range of 600-720 nm. We have used a dose of 200 J/cm^2 at 50 mW/cm^2 for irradiation of cells in culture and 100 J/cm^2

(100 mW/cm^2) for irradiation in animal model experiments. To understand the cellular uptake and localization of **TDC**, we performed fluorescence and confocal microscopic images of **TDC** with SKOV-3 cell lines using blue stain Hoechst 3342 at different conditions. It is interesting to observe that when SKOV-3 cells were incubated with 20 μM **TDC** for 1 h, the cells readily uptake the sensitizer. Moreover, intracellularly, **TDC** showed a high and punctuate fluorescence indicating its probable vesicular/mitochondrial association and also a diffused fluorescence along the membrane periphery as shown in Figure 2. The dye localization to F-actin and to.

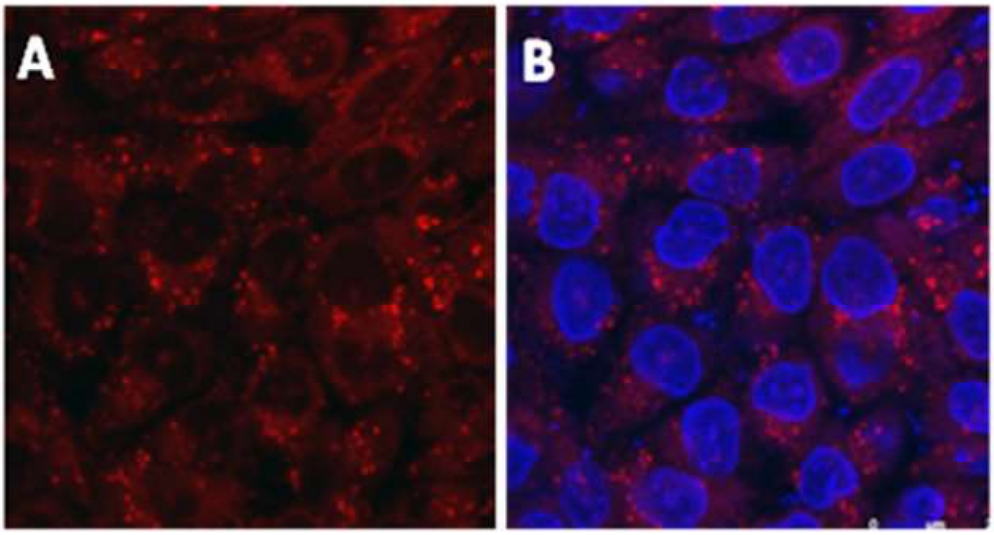

Figure 2. Uptake of **TDC** by SKOV-3 cells. A) Red fluorescence **in SKOV-3 cells** after treatment with 20 μM **TDC** and B) merged image showing SKOV-3 cell nuclei with a vital nuclear dye Hoechst 33342 (blue) and **TDC** (red).

mitochondria has been subsequently confirmed by co-localization experiments using specific probes (Figures 6 and 7). It has been reported earlier, that even low levels of singlet oxygen produced in close proximity to the target organelle such as mitochondria is far more efficient in its phototoxic effects, than a large quantities generated at a distant cellular location.[41] The

proximity of localization of TDC to vital intracellular organelles, could therefore yield more efficient phototoxicity.

Cell viability as measured by 3-(4,5-dimethylthiazol-2-yl)-2,5-diphenyltetrazolium bromide (MTT) assay showed a clear dose dependent photo-toxicity (Figure 3A). We observed a significant loss of viability of SKOV-3 cells at concentrations beyond 10 μM and followed typical biological protocols. Under these experimental conditions, the IC_{50} value of **TDC** was

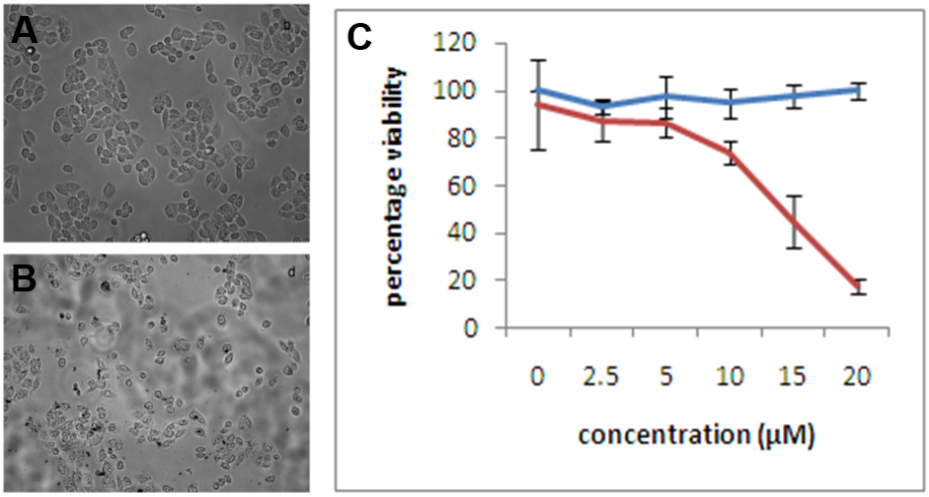

Figure 3. Cytotoxic and phototoxic effects of **TDC:** A) Dark control: SKOV-3 cells treated with **TDC** but not exposed to light and B) cells after photo-irradiation (100X). C) Viability of SKOV-3 cells that were exposed to varied concentrations of **TDC** left unexposed to light (dark control, blue line) and after light exposure (red line); cell viabilities were measured at 24 h after their respective treatments (the results are an average of 3 independent experiments).

calculated to be 11.16±2.08 μM for SKOV-3 cells. **TDC** exhibited excellent photo-toxic effects with the IC_{50} values varying from 4-20 μM depending on the cancer cell line used ((IMR32 (3.5±0.84 μM), MCF7 (4.4±1.62 μM) and MDA MB 231 (6.1±1.16 μM)). Phase contrast

microscopic images of **TDC** treated SKOV-3 cells, in the absence of light exposure, displayed minimal alterations in the cell morphology. However, dye treated cells when exposed to light, displayed extensive changes in cell morphology, indicating cell death).

Further, to understand the dark cytotoxicity and cellular mechanism behind the photodynamic efficacy of **TDC** on SKOV-3 cells, we have analyzed SKOV-3 cells by staining with propidium iodide (PI) and flow cytometric cell cycle analysis (Figure 4).[42] In a typical distribution, sub G1 population represents the hypo-diploid, dead cells. The experimental controls displayed *ca.* 1-7% cells in sub-G1 stage, whereas the cells treated with **TDC** and exposed to light showed a sub-G1 population of *ca.* 60% after 12 h and ca. 77% after 24 h. A gradual shift of cells to sub-G1 population indicates the persistence of photo-induced effects of **TDC** over a period of time. This gradual shift of cells to sub-G1 phase represents the immediate and late events connected to the photodynamic damage of cellular DNA. After 24 h post irradiation, we observed the shift of almost entire population of cells towards sub-G1 phase, indicating an excellent phototoxic effect of **TDC.**

Mode of Cell Death. To understand the mode of phototoxic activity, flow- cytometric analysis was performed on live SKOV-3 cells (both control and **TDC** treated cells) stained with propidium iodide (PI). The control cells (untreated and dark control) showed negligible PI fluorescence (population of cells in M2 window of ~7-9%), whereas the cells treated with **TDC** and exposed to light displayed a very intense fluorescence and showed about *ca.* 80% of the cell

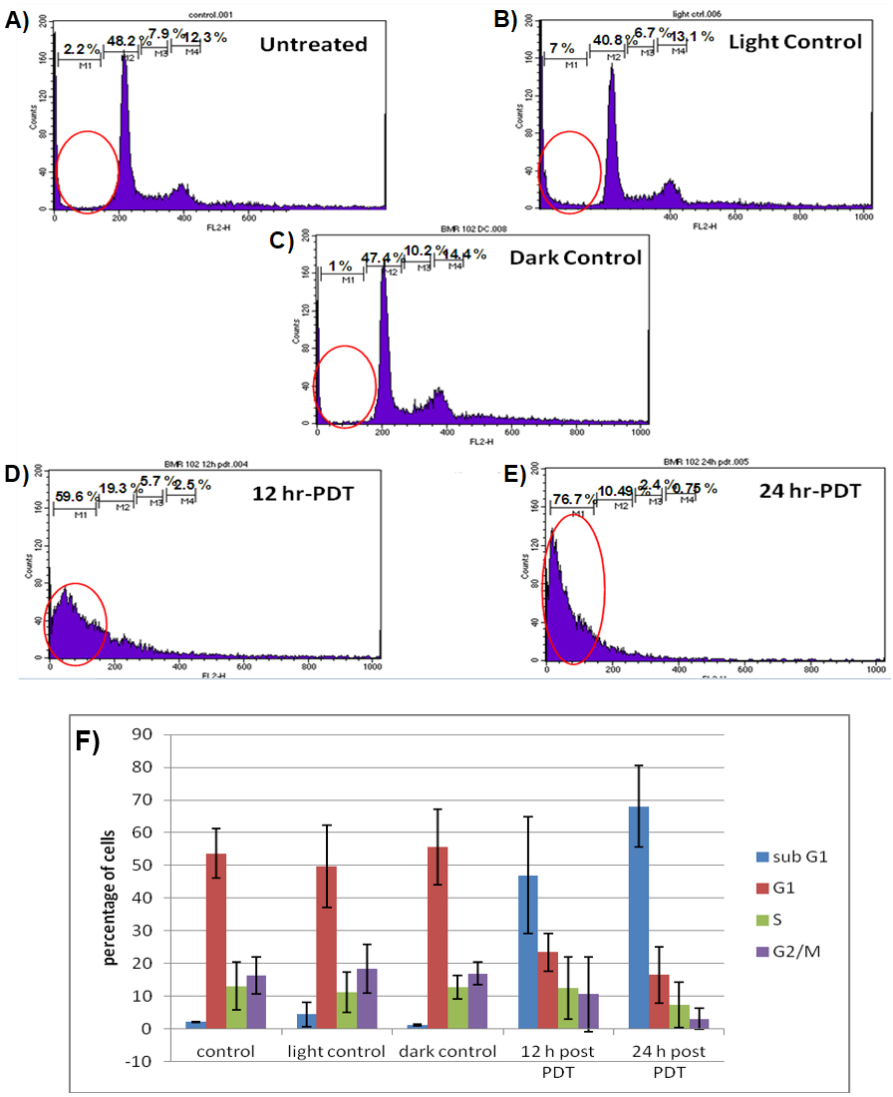

Figure 4. Cell cycle analysis-time dependent phototoxicity of **TDC** (20 μM) in SKOV-3 cells. Flow cytometric analysis shows the percentage of Sub-G1 population (dead) of cells (shown in red circles); A) control (2.2%), B) light control (7%), C) dark control (1%) and post- irradiation (λ_{irr} 600-720 nm; dose 200 J/cm^2 at 50 mW/cm^2) of cells after D) 12 h (60%) and E) 24 h (77%). F) Graphical representation of the cell cycle data

population. These observations clearly demonstrated the loss of cell membrane integrity (Figure 5) and indicated necrosis to be the main mode of phototoxic killing effect of TDC. To have a better understanding in generation of intracellular reactive oxygen species we have used a well-

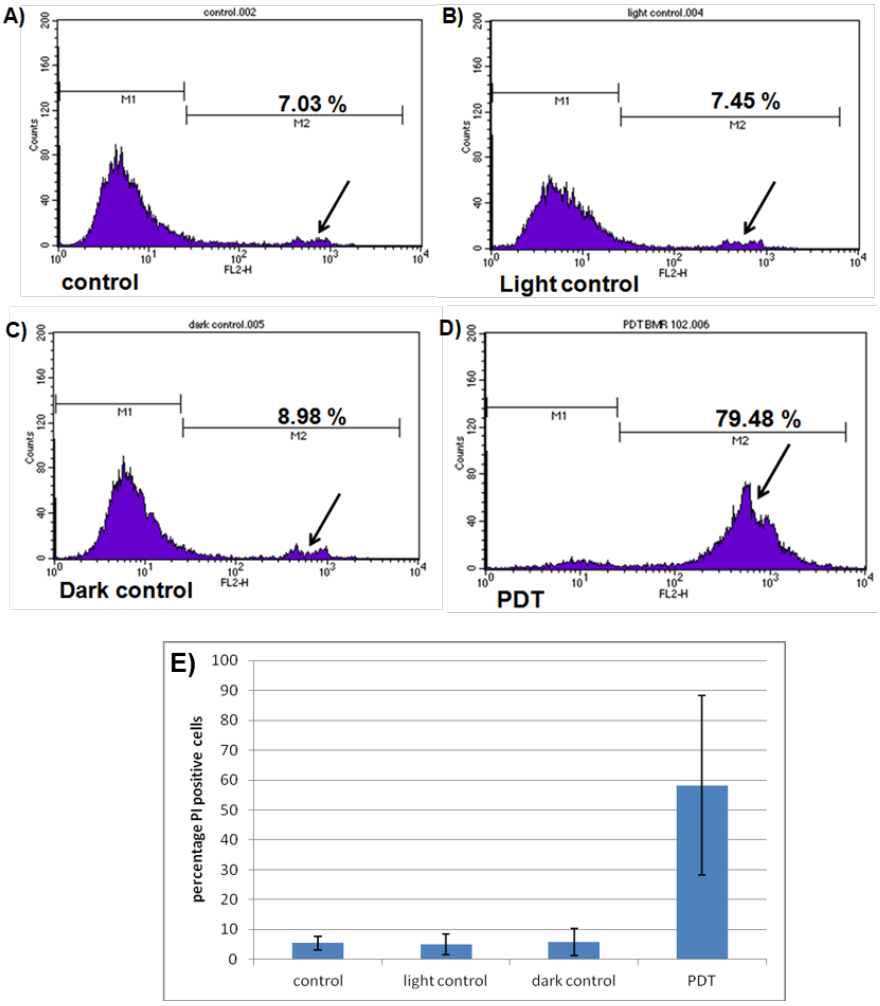

Figure 5. Live cell staining and flow cytometric analysis of control and **TDC** (20 μM) treated SKOV-3 cells with propidium iodide (PI) (10 μg/mL)**.** PI-positive membrane-damaged cells are seen only after photo-irradiation (λ_{irr} 600-720 nm; dose 200 J/cm^2). The percentage of PI positive cells in (denoted by arrows), A) control (7%), B) light control (7.5%), C) dark control (9%) and D) after PDT (79%). E) Graphical representation of the live cell staining with Propidium Iodide.

known fluorescent probe 5-(and-6)-chloromethyl-2′,7′-dichloro-dihydrofluorescein diacetate acetyl ester (CM-H_2DCFDA). To perform CM-H_2DCFDA assay, the human ovarian cancer SKOV-3 cells were treated with **TDC** and irradiated followed by the addition of CM-H_2DCFDA (10 μM) and examined through confocal microscopy. We observed appearance of green fluorescence only in the TDC treated and light exposed cells indicating the generation of ROS, while the untreated or dark control cells showed no fluorescence. A parallel flow cytometric analysis under the same conditions also confirmed that *ca.* 73% of cell population displayed ROS fluorescence only in the cells treated with **TDC** and exposed to light, while the control cells exhibited negligible ROS levels (*ca.* < 1%) (Figure S2, Supporting Information).

In SKOV-3 cells, the actin appears as circularly organized filaments, located near the plasma membrane. Motivated from the live cell propidium iodide (PI) staining experiments, which indicated loss of cell membrane integrity, we analyzed actin cytoskeletal integrity of the SKOV-3 cells before and after the photodynamic treatment using tetramethylrhodamine (TRITC) labeled Phalloidin, an F-actin specific fluorescent probe.[43] The cells treated with **TDC** followed by irradiation showed a complete collapse in F-actin filament network, whereas the control cells remained intact (Figure 6). These observations demonstrated disruption of filamentous actin-cytoskeleton organization in cells. Loss of cytoskeletal integrity could potentially disrupt several physiological functions in the cell that ultimately trigger cell death.[44]

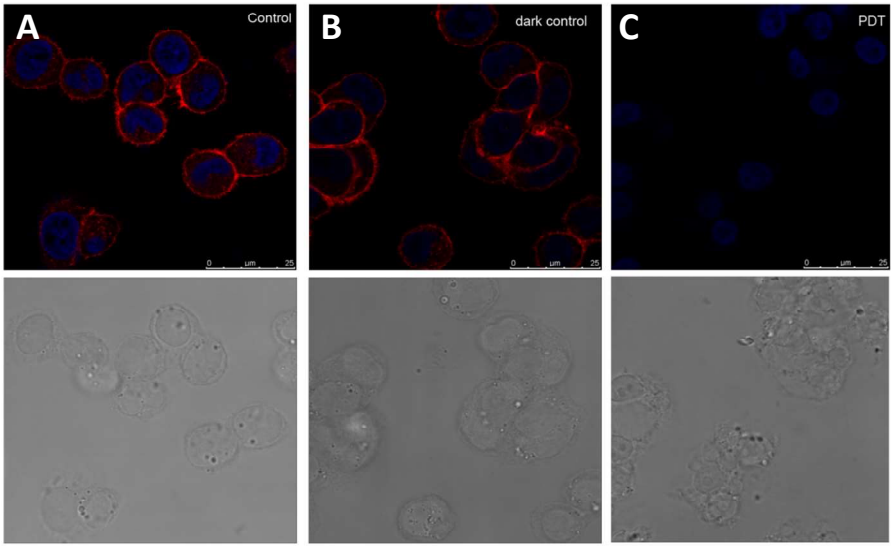

Figure 6. Photodynamic destruction of actin filament organization in SKOV-3 cells. F-actin stained by Phalloidin (red) and the nuclei stained with 4',6-diamidino-2-phenylindole (DAPI) (blue); A) untreated cells, B) cells treated with **TDC** (20 μM) but not exposed to light and C) cells treated with **TDC** (20 μM) and exposed to light (600-720 nm; 200 J/cm^2). Corresponding bright field images are shown in the lower panel.

To understand the mitochondrial integrity, **TDC** treated and light exposed SKOV-3 cells were stained with MitoTracker Red (CMXRos), a fluorophore sensitive to the mitochondrial membrane potential ($\Delta\Psi_m$) (Molecular Probes, OR, USA). The mitochondria of untreated SKOV-3 cells showed typical fibrillar appearance with bright fluorescence denoting intact mitochondrial membranes (Figure 7A). **TDC** treated and light exposed SKOV-3 cells showed a loss of mitochondrial network, which can be clearly evidenced from Figure 7B. Damage to the mitochondrial integrity can lead to cellular events such as cessation of adenosine 5'-triphosphate (ATP) production, release of toxic proteins into cytoplasmic milieu that ultimately trigger cell death.[45,46] These results clearly demonstrate that the **TDC** photodynamically damages cell

membrane, disrupts actin cytoskeletal network and result in the loss of mitochondrial membrane potential (indicating mitochondrial damage). The photoxic killing of SKOV-3 cells by **TDC** is a net destruction of critical cellular organelles and cell death is predominantly considered to be through necrosis or necroptosis. Moreover, the **TDC** showed good photo-stability and its photocytotoxic effects persisted over a period of time, thus probably minimizing the requirement of multiple light exposures.

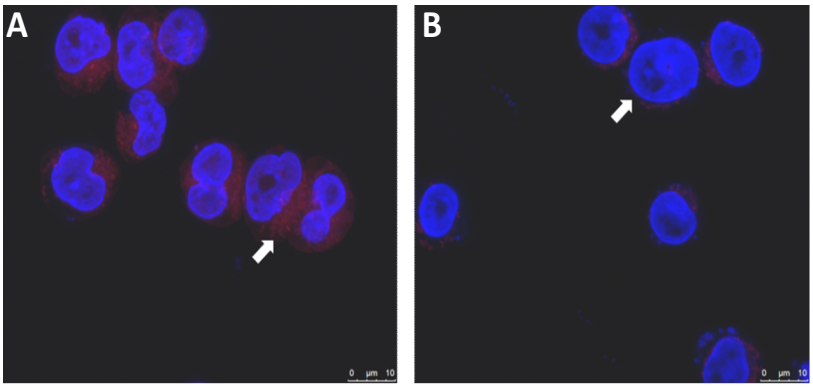

Figure 7. Phototoxic destruction of mitochondria in SKOV-3 cells. Mitochondria was stained by Mitotracker red fluorescent probe (red mesh like structures surrounding the nuclei) and the nuclei were stained with Hoechst 33342 (blue); A) Untreated cells and B) cells treated with **TDC** (20 μM) and exposed to light (600-720 nm; 200 J/cm^2).

Demonstration of *In Vivo* Photodynamic Activity. The excellent photodynamic killing by **TDC** on SKOV-3 cells in culture encouraged us to establish its tumoricidal efficacy *in vivo* using nude mice model. To analyze this, SKOV-3 cells (~3-5 X 10^6 cells, in a final volume of 200 μL) were injected subcutaneously in the dorsal flank of the nude mice and kept for one week in order to develop the tumors. After injecting SKOV-3 cells, the nude mice were divided into two groups. The first group of six animals served as the tumor bearing controls, whereas the second group of animals bearing tumor were treated with **TDC** followed by irradiation. The

sensitizer, **TDC** (in physiological saline) was administered intravenously (20 mg/Kg body weight) to the mice models, anesthetized and were exposed to light (100 J/cm^2 and 100 mW/cm^2) for about 12-18 h post-**TDC** administration. The tumor volumes (TV; mm^3) were monitored for over a period of two weeks and are shown in Figure 8. As per the ethical animal practices, animals with tumor volumes exceeding 10% of the body weight were sacrificed.

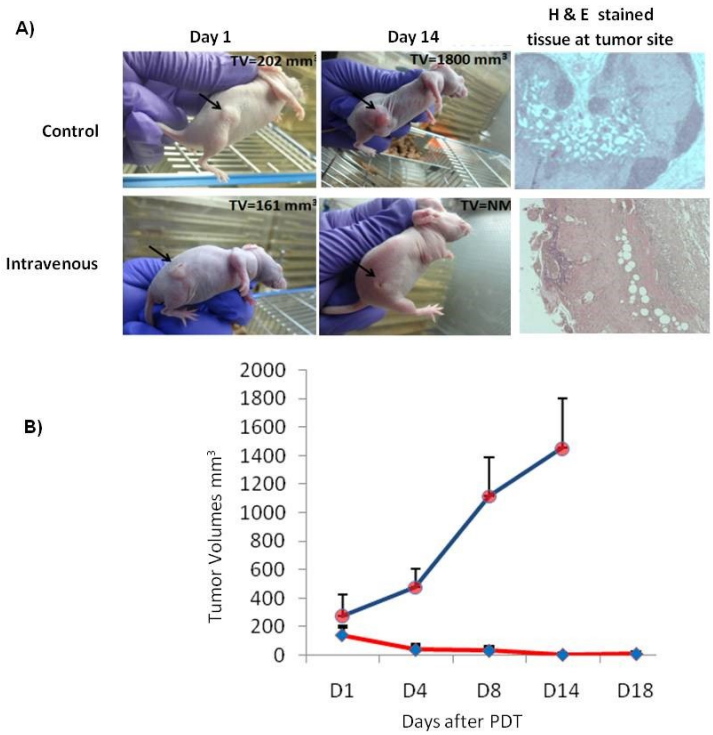

Figure 8. Effect of **TDC** (20 mg/Kg body weight) on tumor progression in nude mice. A) Nude mice bearing SKOV-3 tumors untreated (left) and treated with **TDC** (right) after measuring the tumor volumes (TV) on day 1 and day 14, respectively. The corresponding Hematoxylin & Eosin (H&E) stained tissue sections (biopsied at the site of injection) showing the elimination of neoplastic cells in tumors of mice injected with **TDC** to show the clearance of neoplastic tissues. B) Tumor volumes measured in controls (blue line) and animals (n=6) subjected to PDT (red line) on various days.

The tumor volumes measured on first day (before the administration of **TDC**) and fourteenth day were monitored and are shown in Figure 8A. Interestingly, the tumor volumes were not measurable after fourteen days in animal models when **TDC** treated and exposed to irradiation. The *in vivo* biological experiments clearly indicate that the control animals those shown in left panel exhibited enormous tumor growth, whereas **TDC** treated and light exposed animals showed a dramatic reduction in tumor volumes to below measurable levels, sometimes in a short span of < 14 days without any observable scar at the site of the tumor. For the post experimentation, a small bit of the tissue at the tumor site was biopsied, processed for histology and stained with Hematoxylin as well as Eosin. These tissue sections clearly showed the complete replacement of neoplastic cells with fibrous and other cell types (Figure 8, H & E stained panels on the right side). It can be observed that there is a minimal scarring at the site of the tumor. Uniquely, the photodynamic treatment with the skin in peritumoral area of the animals did not exhibit any sensitivity throughout the experimental period, thereby indicating that **TDC** administration is safer compared to the commercially available photosensitizers.

To determine the *in vivo* cellular localization, tumor bearing animals were injected with **TDC** intra-tumorally and the tumors were biopsied for 12 h post administration, sectioned and analyzed by fluorescence microscopy. We observed that the **TDC** fluorescence (red) is mainly localized in the neoplastic cells (Figure 9), whereas the cells of fibrous tissue and that of stroma (nuclei stained blue) did not show red fluorescence. Selective localization of **TDC** and other photosensitizers in cancer cells is a subject of immense interest. It is hypothesized that p-glycoproteins, which are responsible for drug efflux, play an important role in the selective cellular retention of the photosensitizers.

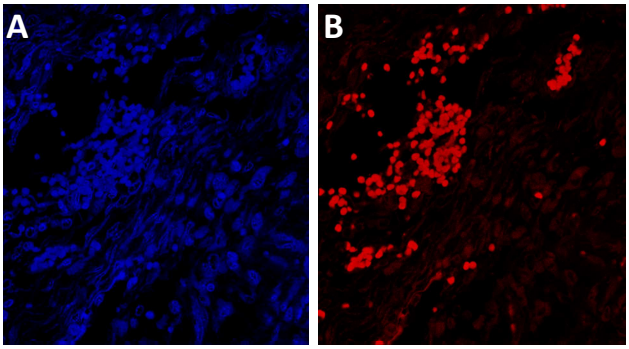

Figure 9. Intra-tumoral localization of **TDC** (20 mg/Kg body weight) in nude mice. Biopsies from the tumors bearing animals injected with **TDC** intra-tumorally were sectioned and visualized by fluorescence microscopy. A) DAPI stained section shows nuclei from both SKOV-3 cancer cells and stromal tissue nuclei (blue) and B) **TDC** visualized as bright red fluorescence, the sensitizer is localized in the neoplastic cells only.

To understand the effect of **TDC** on non-target organs, we examined the systemic effects of PDT in biopsied and sectioned tissues of various body parts such as liver, kidney, spleen, heart, lung of the animal models. The post-PDT treatment in these tissues under various conditions such as untreated, dark control and with **TDC** were stained with standard Hematoxylin and Eosin are shown in Figure 10. These studies clearly showed that the cellular morphology of these organs remained intact without any detectable tissue pathology implying that **TDC** does not affect the normal tissue, but uniquely localize only in the neoplastic tissue and damage it selectively.

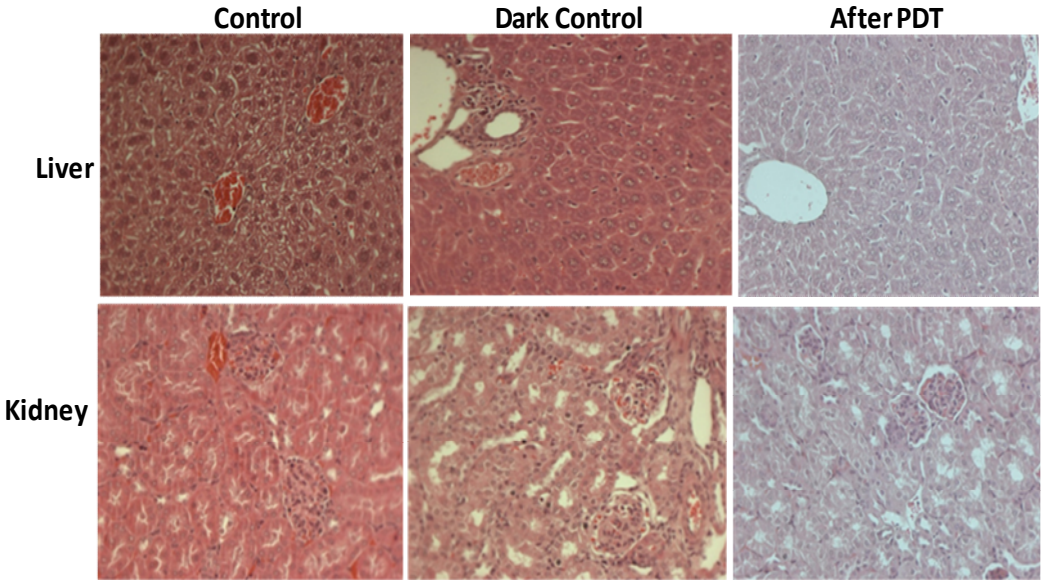

Figure 10. The cytomorphology of liver and cytopathological changes of kidney tissues show the photodynamic effect of **TDC** (20 mg of **TDC**/Kg body weight of nude mice). Representative animal sections of the liver and kidney tissues under various conditions (control, dark control and after PDT of treatment light dose; 100 J/cm^2; 600-720 nm) are shown after staining with standard Hematoxylin & Eosin.

CONCLUSION

In conclusion, the dihydroxychlorin, **TDC** described herein exhibited high solubility in biological media and excellent quantum yields of triplet excited state (0.84 ± 0.02) and singlet oxygen generation (0.80 ± 0.03). Our *in vitro* photodynamic investigations have indicated that **TDC** localizes selectively in neoplastic cells and the biological activity involved predominantly ROS as the reactive intermediates. Interestingly, **TDC** induces a severe intracellular oxidative photodynamic damage in ovarian cancer cells through the destruction of cellular organelles such as cell membrane, actin cytoskeletal and mitochondria. Moreover, the absence of any detectable

changes in the apoptotic markers such as caspase-3 clearly indicates that the mechanism of cell death is predominantly through a necrosis pathway. Uniquely, **TDC** exhibited negligible dark cytotoxicity and excellent photodynamic activity both in cell culture and nude mice animal models. The ease of synthesis, chemical purity, aqueous solubility, high optical absorption in the photodynamic window, efficient generation of triplet and singlet oxygen species, excellent *in vitro* and *in vivo* photodynamic activity and non-toxic effects on non-target tissues such as liver, kidney, spleen, heart etc makes **TDC** a promising sensitizer for photodynamic therapy of cancer.

EXPERIMENTAL SECTION

General Techniques. The general techniques and equipments employed were described elsewhere.[47-50] All the compounds synthesized were purified (≥95%) through re-crystallization and characterized based on elemental analysis and spectral evidence. ^{1}H and ^{13}C NMR spectra were measured on a 300 or 500 MHz Bruker advanced DPX spectrometer. The IR spectra were recorded on a Perkin Elmer Model 882 infrared spectrometer. The electronic absorption spectra were recorded on a Shimadzu UV-VIS-NIR spectrophotometer and fluorescence spectra were recorded on a SPEX-Fluorolog F112X spectrofluorimeter. The biological properties of the sensitizer have been investigated using a human ovarian cancer cell line SKOV-3. For the evaluation of phototoxicity, we have used a tunable, commercially available light source, Waldman PDT 1200L (Germany) having the emission spectrum in the range of 600-750 nm. We have used light dose of 200 J/cm^2; 50 mW/cm^2 for *in vitro* irradiation of cells in culture and 100 J/cm^2; 100 mW/cm^2 for *in vivo* irradiation, in animal model experiments. These cell culture studies were performed on FACS Star (Becton Dickinson, USA) and Laser Scanning

Microscopy (Leica SP8, Germany), cytotoxicity /phototoxicity analyses were done using Elisa Plate Reader (Molecular Devices, USA).

Materials. 3,4-Dimethoxybenzaldehyde, pyrrole, trifluoroacetic acid, DDQ, dulbecco's modified eagle medium (DMEM), dimethyl sulphoxide (DMSO), propidium iodide, Hoechst dye, and RNAse were purchased from Aldrich and used as received. 1,3-Diphenylisobenzofuran (DPBF) was recrystallized from a mixture (1:3) of methanol and acetone. SKOV-3 cells were procured from ATCC (USA). DMEM, fetal calf serum and antibiotics, 3-(4,5-dimethyl-thiazol-2-yl)-2,5-diphenyltetrazolium bromide (MTT) and propidium Iodide were from Sigma-Aldrich, USA, CM-H_2DCFDA and Mitotracker Red CMXRos were procured from Molecular Probes, USA.

Chemical Synthesis. Step 1. Synthesis of 3.4-Dimethoxyphenylporphyrin. The synthesis of the porphyrin derivative was achieved through the modified procedure of Lindsey.[36] 3,4-Dimethoxybenzaldehyde (0.009 mol) and pyrrole (0.6 mol) were dissolved in distilled dichloromethane (500 mL) and trifluoroacetic acid (~0.2 mL) was added and kept stirring for ~3-5 h at room temperature and under argon atmosphere. 2,3-Dichlorodicyanobenzoquinone (1.2 eq) was then added and the reaction was allowed to continue for 2 h more. 3,4-Dimethoxyphenylporphyrin was purified from the reaction mixture by sequentially passing through basic alumina and silica (100-200 mesh) column using dichloromethane as the mobile phase. The purple colored product was collected and concentrated by vacuum drying.

Step 2. Synthesis of 5,10,15,20-Tetrakis(3,4-dimethoxyphenyl)chlorin. 3,4-Dimethoxyphenyl-porphyrin (3.2 mmol) and *p*-tosylhydrazine (32 mmol) were dissolved in dry pyridine (500 mL) and activated potassium carbonate (1.3 mmol) was added. The reaction mixture was allowed to reflux at 120 ºC under argon atmosphere for 24 h. After 2 h, the reaction

was monitored by UV-visible spectroscopy (the peak at 650 nm corresponding to chlorin). After completion of the reaction, the reaction mixture was cooled and extracted using dichloromethane. The organic layer was concentrated, dried and was poured onto a column of alumina (50 mm diameter, 150 mm length) and eluted with dichloromethane. The solvent was removed under reduced pressure to give a black solid, which was then subjected to column chromatography using over silica gel. Elution of the column with chloroform gave the chlorin derivative. Yield: (83%), mp > 300 ºC, purity ≥95%, IR (KBr): ν_{max} 3324, 2821, 1680, 1516, 1261, 1246, 1230, 1138, 1028 cm^{-1}. ^{1}H NMR (300 MHz, $CDCl_3$, TMS): δ (ppm) -1.44 (s, 2H), 3.95 (s, 12H), 4.11 (s, 6H), 4.14 (s, 6H), 4.2 (s, 4H), 7.16 (t, 4H, J=15 Hz), 7.39 (d, 4H, J= 5 Hz), 7.67 (d, 4H, J=5 Hz), 8.24 (d, 2H, J=15 Hz), 8.48 (s, 2H), 8.64 (d, 2H, J= 5 Hz). ^{13}C NMR (125 MHz, $CDCl_3$): δ (ppm) 206.9, 167.7, 152.6, 148.7, 147.1, 140.97, 135.6, 134.7, 131.8, 128.0, 126.6, 124.6, 123.3, 122.3, 117.6, 109.4, 77.0, 56.1.FAB-MS: m/z calculated 857.4; found 857.35 (M^+).

Step 3. Synthesis of 5,10,15,20-Tetrakis(3,4-dihydroxyphenyl)chlorin (TDC). Boron tribromide (7.4 mmol) in dry dichloromethane (10 mL) was cooled to -78 ºC and was added 5,10,15,20-tetrakis(3,4-dimethoxyphenyl)chlorin (0.3 mmol) in dry dichloromethane (10 mL), over a period of 20 min. The mixture was stirred for 2 h at -78 ºC and then for 12 h at 25 ºC. After cooling to 0 ºC on an ice bath, methanol was added to quench any excess of boron tribromide.Triethylamine was then added to neutralize the reaction mixture and concentrated under reduced pressure to give an amorphous purple solid. The solid thus obtained was recrystallized from a mixture of methanol and chloroform to obtain dihydroxychlorin derivative, **TDC**. Yield: (85%), mp > 300 ºC, purity ≥95%, IR (KBr): ν_{max} 3187, 2694, 1577, 1525, 1512, 1500, 1431, 1354, 1255, 1112, 935 cm^{-1}. ^{1}H NMR (300 MHz, DMSO-d_6, TMS): δ (ppm) -1.43

(s, 2H), 4.2 (s, 4H), 7.12 (t, 4H, J=20 Hz), 7.17 (d, 2H, J=10 Hz), 7.28 (s, 2H), 7.39 (d, 2H, J=10 Hz), 7. 53 (s, 2H), 8.29 (d, 2H, J=5 Hz), 8.48 (s, 2H), 8.68 (d, 2H, J=5 Hz). ^{13}C NMR (125 MHz, DMSO-d_6): δ (ppm) 167.8, 152.6, 145.0, 144.6, 140.7, 137.8, 135.3, 134.4, 131.2, 127.5, 125.8, 123.7, 122.3, 121.4, 119.3, 112.1, 99.8, 48.13. FAB-MS: m/z calculated: 745.2; found 745.31 (M^+).

Cell Culture Analysis. The human ovarian carcinoma cell line SKOV-3 was maintained in DMEM containing Penicillin, Streptomycin and Gentamycin (100 units, 100 µg and 50 µg/ mL respectively) supplemented with 10 % fetal calf serum under standard culture conditions (37 ºC , 5 % CO_2 and 95% humidity). The cells were sub-cultured once in two days.

Cell Cycle Analysis by Flow Cytometry. SKOV-3 cells in T-25 flasks were treated with **TDC** (20 µM) and either exposed to light or left unexposed, were harvested at pre-determined times and washed in ice-cold PBS. The cells were re-suspended in PBS and fixed in 1 mL ice-cold 70% ethanol and left overnight at 4 ºC. After another PBS wash, cells were stained with propidium iodide (60 µg/mL) and DNAse free ribonuclease A (0.2 mg/mL) and incubated for 30 min at 37 ºC. The cells were analyzed for propidium iodide fluorescence using a flow cytometer equipped with an excitation laser at 488 nm. The cell cycle analysis was done as per the standard procedure and the percent population of cells representing different phases of cell cycle (by gating cells using width and area parameters) was estimated.

Flow Cytometric Analysis of Live SKOV-3 Cells Stained with Propidium Iodide. Propidium iodide being membrane impermeant dye is excluded by living cells, but readily enters dead and membrane-compromised cells and emits a strong fluorescent signal when bound to DNA. SKOV-3 cells were subjected to different treatments as described, harvested and washed

with phosphate buffered saline (PBS) and stained with propidium iodide (10 μg/mL) for 20 min and analyzed by flow cytometry.

Mitochondrial Membrane Potential. Control cells and cells after PDT were treated with 200 nM of Mitotracker Red CMXRos and incubated at 37 ºC for 30 min. The cells were then fixed in formaldehyde, counterstained with DAPI and visualized by confocal microscopy.

Nude Mice Xenograft Models of Ovarian Cancer. All experiments were carried out in accordance with the guidelines of Institutional Animal Ethics Committee (CCMB, Hyderabad, India). Approximately 3-4 million SKOV-3 cells were injected subcutaneously into the flank region of 6-8 week old *FoxN1* nude mice (20-25 g). Tumor dimensions were measured using a digital calipers and the volumes were calculated using the formula $V=LW^2/2$ (where V= volume; L= length of the tumor; W=width of the tumor). When tumor volumes reached approximately 100 -150 mm^3, the mice were randomly divided into four groups of six animals each, the untreated control group, the light control group (only exposed to light), the dark control group (**TDC** was administered, but not exposed to light) and the PDT group (administration of **TDC** followed by irradiation for 24 h).

TDC was administered intravenously (dark control group and PDT group) at 20 mg/Kg body weight. The animals (PDT group) were subjected to irradiation 24 h after administration of **TDC**. For animal experiments, the irradiation parameters were 100 J/cm^2 and 100 mW/cm^2. Prior to irradiation, the nude mice were anesthetized with ketamine (60 mg/Kg) and xylazine (8 mg/Kg) given intraperitoneally. Only the tumor region was exposed to light while the rest of the animal was shielded. Tumor growth was assessed by monitoring its volume. For histopathology studies, animals were euthanized according to IAEC protocols. Tumor, liver, spleen kidney, heart and lung were collected, fixed in buffered formalin, dehydrated and paraffin-embedded.

The tissues were sectioned at 5 μm thickness and stained with Hematoxylin and eosin A contiguous section was used to study the intratumoral localization of **TDC**.

Staining of F-actin. Untreated dark control or photodynamically treated SKOV-3 cells (grown on cover slips) were fixed with 4% paraformaldehyde in phosphate buffered saline washed and permeabilized with 0.1% Triton X100. Following the permeabilization, cells were treated with TRITC-Phalloidin (Sigma-Aldrich, USA) at a dilution of 1:50 for 1 h. Finally, the cells were counterstained with DAPI and visualized by confocal microscopy.

Uptake and Intracellular Localization of TDC by SKOV-3 Cells. SKOV-3 cells, grown in chambered glass slides were treated with 20 μM **TDC** for 1 h. The slides were then rinsed with phosphate buffered saline (PBS), treated with Hoechst 33342 (1 μg/mL) and visualized by confocal microscopy. **TDC** show red fluorescence and the nuclei appear blue.

ASSOCIATED CONTENT

Supporting Information Available: General methods, quantification of triplet states and singlet oxygen quantum yields, Figures S1-S2 and Table S1 showing the photophysical and photobiological properties of **TDC** are summarized. Molecular formula strings file uploaded separately. This material is available free of charge via the internet at http://pubs.acs.org.

AUTHOR INFORMATION

Corresponding Author

D. Ramaiah: ORCID # 0003-1388-4768

*E-mail: rama@neist.res.in or d.ramaiah@gmail.com.

Notes

The authors declare no competing financial interests.

ACKNOWLEDGMENTS

The authors acknowledge the financial support from the Department of Biotechnology (BMB/2015/53) and Department of Science and Technology (SR/S5/MBD-01C/2007), Government of India. CMR and TKC acknowledge the DST, Sir JC Bose National Fellowship. The authors acknowledge the help by Dr. Jerald Mahesh Kumar, Veterinary Pathologist and Officer-in-charge, Animal House Facility, CCMB, for his inputs in histopathological analyses.

AUTHOR CONTRIBUTIONS

Dr. B. Marydasan and Dr. B. Madhuri have contributed equally to this manuscript. Dr. B. Marydasan, Dr. M. Viji, Dr. S. C. Karunakaran, Dr. T. K. Chandrashekar and Dr. D. Ramaiah, participated in the synthesis and photophysical characterization of **TDC**, while Dr. B. Madhuri, J. Jose, S. Cherukommu, Dr. Ch Mohan Rao and Dr. K Sridhar Rao, participated in evaluation of photobiological properties and animal experimentation. Dr. K. Sridhar Rao, Dr. Ch. Mohan Rao and Dr. Ramaiah are also involved in collation of data, data analysis and manuscript preparation.

ABBREVIATIONS USED

PDT, photodynamic therapy; NIR, near-infrared; HPD, hematoporphyrin derivative; TDC, 5,10,15,20-tetrakis(3,4-dihydroxyphenyl)chlorin; MTT, 3-(4,5-dimethylthiazol-2-yl)-2,5-diphenyltetrazolium bromide; PI, propidium iodide; DAPI, 4',6-diamidino-2-phenylindole; DPBF, diphenylisobenzofuran; TRITC, tetramethylrhodamine; ROS, reactive oxygen species.

REFERENCES

(1) Singh, S.; Aggarwal, A.; Bhupathiraju, D. K.N. V. S.; Arianna, G.; Tiwari, K.; Drain, C. M. Glycosylated Porphyrins, Phthalocyanines, and Other Porphyrinoids for Diagnostics and Therapeutics. *Chem. Rev.* **2015**, *115*, 10261-10306.

(2) Lai, Y. C.; Su, S. Y.; Chang, C. C. Special Reactive Oxygen Species Generation by a Highly Photostable Bodipy-Based Photosensitizer for Selective Photodynamic Therapy. *ACS Appl. Mater. Interfaces* **2013**, *5*, 12935-12943.

(3) Dharmaraja, A. T. Role of Reactive Oxygen Species (ROS) in Therapeutics and Drug Resistance in Cancer and Bacteria. *J. Med. Chem.* **2017***, 60*, 3221-3240.

(4) Durantini, A. M.; Greene, L. E.; Lincoln, R.; Martínez, S. R.; Cosa, G. Reactive Oxygen Species Mediated Activation of a Dormant Singlet Oxygen Photosensitizer:From Autocatalytic Singlet Oxygen Amplification to Chemicontrolled Photodynamic Therapy. *J. Am. Chem. Soc.* **2016**, *138*, 1215-1225.

(5) Esemoto, N. N.; Yu, Z., Wiratan, L.; Satraitis, A.; Ptaszek, M. Bacteriochlorin Dyads as Solvent Polarity Dependent Near-Infrared Fluorophores and Reactive Oxygen Species Photosensitizers. *Org. Lett*. **2016**, *18*, 4590-4593.

(6) Soares, A. R. M.; Neves, M. G. P. M. S.; Tomé, A. C.; Cruz, M. C. I.; Zamarrón, A.; Carrasco, E.; González, S.; Cavaleiro, J. A. S.; Torres, T.; Guldi, D. M.; Juarranz, A. Glycophthalocyanines as Photosensitizers for Triggering Mitotic Catastrophe and Apoptosis in Cancer Cells. *Chem. Res. Toxicol.* **2012***, 25*, 940-951.

(7) Machacek, M.; Cidlina, A.; Novakova, V.; Svec, J.; Rudolf, E.; Miletin, M.; Kučera, R.; Simunek, T.; and Zimcik, P. Far-Red-Absorbing Cationic Phthalocyanine Photosensitizers:

Synthesis and Evaluation of the Photodynamic Anticancer Activity and the Mode of Cell Death Induction. *J. Med. Chem.* **2015**, *58*, 1736-1749.

(8) Thomas, A. P.; Saneesh Babu, P. S.; Nair, A. S.; Ramakrishnan, S.; Ramaiah, D.; Chandrashekar, T. K.; Srinivasan, A.; Pillai, M. R. *m*eso-Tetrakis(p-sulfonatophenyl)n-Confused Porphyrin Tetrasodium Salt: A Potential Sensitizer for Photodynamic Therapy. *J. Med. Chem.* **2012**, *55*, 5110-5120.

(9) Castano, A. P.; Demidova, T. N.; Hamblin, M. R. Mechanisms in Photodynamic Therapy: Part One-Photosensitizers, Photochemistry and Cellular Localization. *Photodiagnosis Photodyn Ther.* **2004**, *1*, 279-293.

(10) Liu, S.; Brown, C. W.; Berlin, K. D.; Dhar, A.; Guruswamy, S.; Brown, D.; Gardner, G. J.; Birrer, M. J.; Benbrook, D. M. Synthesis of Flexible Sulfur-Containing Heteroarotinoids that Induce Apoptosis and Reactive Oxygen Species with Discrimination between Malignant and Benign Cells. *J. Med. Chem.* **2004**, *47*, 999-1007.

(11) Yu, Z.; Sun, Q.; Pan, W.; Li, Na.; Tang, B. A Near-Infrared Triggered Nanophotosensitizer Inducing Domino Effect on Mitochondrial Reactive Oxygen Species Burst for Cancer Therapy. *ACS Nano* **2015**, *9*, 11064-11074.

(12) Dolmans, D. E.; Fukumura, D.; Jain, R. K. Photodynamic Therapy for Cancer. *Nat. Rev. Cancer.* **2003**, *3*, 380-387.

(13) Celli, J. P.; Spring, B. Q.; Rizvi, I.; Evans, C. L.; Samkoe, K. S.; Verma, S.; Pogue, B. W.; Hasan, T. Imaging and Photodynamic Therapy: Mechanisms, Monitoring, and Optimization. *Chem. Rev.* **2010**, *110*, 2795-2838.

(14) Chen, W.; Balakrishnan, K.; Kuang, Y.; Han, Y.; Fu, M.; Gandhi, V.; Peng, X. Reactive Oxygen Species (ROS) Inducible DNA Cross-Linking Agents and Their Effect on Cancer Cells and Normal Lymphocytes. *J. Med. Chem.* **2014**, *57*, 4498-4510.

(15) Lee, B. S.; Amano, T.; Wang, H. Q.; Pantoja, J. L.; Yoon, C. W.; Hanson, C. J.; Amatya, R.; Yen, A.; Black, K. L.; Yu, J. S. Reactive Oxygen Species Responsive Nano-prodrug to Treat Intracranial Glioblastoma. *ACS Nano* **2013**, *7*, 3061-3077.

(16) Richard, S.; Saric, A.; Boucher, M.; Slomianny, C.; Geffroy, F.; Mériaux, S.; Lalatonne, Y.; Petit, P. X.; Motte, L. Antioxidative Theranostic Iron Oxide Nanoparticles Toward Brain Tumors Imaging and ROS Production. *ACS Chem. Biol.* **2016**, *11*, 2812-2819.

(17) Yi, X.; Wang, F. L.; Qin, W.; Yang, X.; Yuan, J. Near-Infrared Fluorescent Probes in Cancer Imaging and Therapy: An Emerging Field. *Int J Nanomedicine.* **2014***, 9*, 1347-1365.

(18) Yuan, A.; Wu, J.; Tang, X.; Zhao, L.; Xu, F.; Hu, Y. Application of Near-Infrared Dyes for Tumor Imaging, Photothermal, and Photodynamic Therapy. *J. Pharm. Sci.* **2012***, 102*, 6-28.

(19) Mishra, C. B.; Mongre, R. K.; Kumari, S.; Jeong, D. K.; Tiwari, M. Novel Triazole-Piperazine Hybrid Molecules Induce Apoptosis *via* Activation of the Mitochondrial Pathway and Exhibit Antitumor Efficacy in Osteosarcoma Xenograft Nude Mice Model. *ACS Chem. Biol.* **2017**, *12*, 753-768.

(20) Karunakaran, S. C.; Saneesh Babu, P. S.; Madhuri, B.; Betsy, M.; Paul, A. K.; Nair, A. S.; Rao, K. S.; Srinivasan, A.; Chandrashekar, T. K.; Rao, M. Ch.; Pillai, R.; Ramaiah, D. *In Vitro* Demonstration of Apoptosis Mediated Photodynamic Activity and NIR Nucleus Imaging Through a Novel Porphyrin. *ACS Chem. Biol*. **2013**, *8*, 127-132.

(21) Jayaram, D. T.; Romero, S. R.; Shankar, B. H.; Garrido, C.; Rubio, N.; Sanchez-Cid, L.; Gómez, S. B.; Blanco, J.; Ramaiah, D. *In Vitro* and *In Vivo* Demonstration of Photodynamic

Activity and Cytoplasm Imaging Through TPE Nanoparticles. *ACS Chem. Biol.* **2016**, *11*, 104-112.

(22) Sehgal, I.; Vazquez, M. S.; Vicente, M. G. H. Photoinduced Cytotoxicity and Biodistribution of Prostate Cancer Cell-Targeted Porphyrins. *J. Med. Chem.* **2008**, *51*, 6014-6020.

(23) Detty, M. R.; Gibson, S. L.; Wagner, S. J. Current Clinical and Preclinical Photosensitizers for Use in Photodynamic Therapy. *J. Med. Chem.* **2004**, *47*, 3897-3915.

(24) Jiang, F.; Robin, A. M.; Katakowski, M.; Tong, L.; Espiritu, M.; Singh, G.; Chopp, M. Photodynamic Therapy with Photofrin in Combination with Buthionine Sulfoximine (BSO) of Human Glioma in the Nude Rat. *Lasers Med. Sci.* **2003**, 18, 128-133.

(25) Schweitzer, V. G. Photofrin-Mediated Photodynamic Therapy for Treatment of Early Stage Oral Cavity and Laryngeal Malignancies. *Lasers Surg. Med.* **2001**, *29*, 305-313.

(26) Basu, U.; Khan, I.; Hussain, A.;, Kondaiah, P.; Chakravarty, A. R. Photodynamic Effect in Near-IR Light by a Photocytotoxic Iron(III) Cellular Imaging Agent. *Angew. Chem., Int. Ed.* **2012**, *51*, 2658-2661.

(27) Wainwright, M. Photodynamic Therapy: The Development of New Photosensitisers. *Anticancer Agents Med. Chem.* **2008,** *8*, 280-291.

(28) Lovell, J. F.; Liu, T. W. B.; Chen, J.; Zheng, G. Activatable Photosensitizers for Imaging and Therapy. *Chem. Rev.* **2010**, *110*, 2839-2857.

(29) Varamo, M.; Loock, B.; Maillard, P.; Grierson, D. S. (2007) Development of Strategies for the Regiocontrolled Synthesis of meso-5,10,20-Triaryl-2,3-Chlorins. *Org. Lett.* **2007**, *9*, 4689-4692.

(30) Reidy, K.; Campanile, C.; Muff, R.; Born, W.; Fuchs, B. *m*-THPC-Mediated Photodynamic Therapy is Effective in the Metastatic Human 143B Osteosarcoma Cells. *Photochem. Photobiol.* **2012**, *88*, 721-727.

(31) Ethirajan, M.; Chen, Y.; Joshi, P.; Pandey, R. K. The Role of Porphyrin Chemistry in Tumor Imaging and Photodynamic Therapy. *Chem. Soc. Rev.* **2011,** *40*, 340-362.

(32) O'Connor, A. E.; Gallagher, W. M.; Byrne, A. T. Porphyrin and Nonporphyrin Photosensitizers in Oncology: Preclinical and Clinical Advances in Photodynamic Therapy. *Photochem. Photobiol*. **2009**, *85*, 1053-1074.

(33) Senge, M. O.; Brandt, J. C. Temoporfin (Foscan®, 5,10,15,20-Tetra(m-hydroxyphenyl)chlorin) - A Second-Generation Photosensitizer. *Photochem. Photobiol*. **2011**, *87*, 1240-1296.

(34) Banfi, S.; Caruso, E.; Buccafurni, L.; Murano, R.; Monti, E.; Gariboldi, M.; Papa, E.; Gramatica, P. Comparison Between 5,10,15,20-Tetraaryl- and 5,15-Diarylporphyrins as Photosensitizers: Synthesis, Photodynamic Activity, and Quantitative Structure-Activity Relationship Modeling. *J. Med. Chem.* **2006**, *49*, 3293-3304.

(35) Hong, E. J.; Choi, D. G.; Shim, M. S. Targeted and Effective Photodynamic Therapy for Cancer Using Functionalized Nanomaterials. *Acta Pharm. Sin. B.* **2016**, *6*, 297-307.

(36) Lindsey, J. S. Synthesis of *meso*-Substituted Porphyrins. *The Porphyrin Handbook. Academic Press,* San Diego. **2000**, *1*, 45-118.

(37) Joseph, J.; Eldho, N. V.; Ramaiah, D. Control of Electron-Transfer and DNA Binding Properties by the Tolyl Spacer Group in Viologen Linked Acridines. *J. Phys. Chem. B.* **2003***, 107*, 4444-4450.

(38) Adarsh, N.; Shanmugasundaram, M.; Avirah, R. R.; Ramaiah, D. Aza-Bodipy Derivatives: Enhanced Quantum Yields of Triplet Excited States and the Generation of Singlet Oxygen and Their Role as Facile Sustainable Photooxygenation Catalysts. *Chem. Eur. J.* **2012**, *18*, 12655-12662.

(39) Mathai, S.; Smith, T. A.; Ghiggino, K. P. Singlet Oxygen Quantum Yields of Potential Porphyrin-Based Photosensitisers for Photodynamic Therapy. *Photochem. Photobiol. Sci.* **2007**, *6*, 995-1002.

(40) Sakamoto, K.; Kato, T.; Kawaguchi, T.; Ohno-Okumura, E.; Urano, T.; Yamaoka, T.; Suzuki, S.; Cook, M. J. Photosensitizer Efficacy of Non-Peripheral Substituted Alkylbenzopyridoporphyrazines for Photodynamic Therapy of Cancer. *J. Photochem. Photobiol. A: Chem.* **2002**, *153*, 245-253.

(41) Rubio, N.; Fleury, S. P.; Redmond, R. W. Spatial and Temporal Dynamics of *In Vitro* Photodynamic Cell Killing: Extracellular Hydrogen Peroxide Mediates Neighboring Cell Death. *Photochem. Photobiol. Sci.* **2009**, *8*, 457-464.

(42) Crowley, L. C.; Marfell, B. J.; Scott, A. P.; Waterhouse, N. J. Quantitation of Apoptosis and Necrosis by Annexin V Binding, Propidium Iodide Uptake, and Flow Cytometry. *Cold Spring Harb. Proto*c. **2016**, *11*, 953-956.

(43) Sawai, H.; Domae, N. Discrimination Between Primary Necrosis and Apoptosis by Necrostatin-1 in Annexin V-Positive/propidium Iodide-Negative Cells. *Biochem. Biophys. Res. Commun.* **2011,** *411*, 569-573.

(44) Morley, S. C.; Sun, G. P.; Bierer, B. E. Inhibition of Actin Polymerization Enhances Commitment to and Execution of Apoptosis Induced by Withdrawal of Trophic Support. *J. Cell. Biochem.* **2003**, *88*, 1066-1076.

(45) Teiten, M. H; Marchal, S.; D'Hallewin, M. A.; Guillemin, F.; Bezdetnaya, L. Primary Photodamage Sites and Mitochondrial Events after Foscan® Photosensitization of MCF-7 Human Breast Cancer Cells. *Photochem. Photobiol*. **2003**, *78,* 9-14.

(46) Weinberg, S. M.; Chandel, N. S. Targeting Mitochondria Metabolism for Cancer Therapy. *Nat. Chem. Biol*. **2014**, *11*, 9-15.

(47) Bhattacharyya, K.; Ramaiah, D.; Das, P. K.; George, M. V. A Laser Flash Photolysis Study of 2,6-Dimethyl-3,5-diphenyl-4-pyrone and Related Chromones. Evidence for Triplet State Structural Relaxation from Quenching Behavior, *J. Phys. Chem*. **1986**, *90*, 5984-5989.

(48) Tyagi, N.; Viji, M.; Karunakaran, S. C.; Varughese, S.; Ganesan, S.; Priya, S.; Saneesh Babu, P. S.; Nair, A. S.; Ramaiah, D. Enhancement in Intramolecular Interactions and *In Vitro* Biological Activity of a Tripodal Tetradentate System Upon Complexation. *Dalton Trans*. **2015**, *44*, 15591-15601.

(49) Adam, W.; Cadet, J.; Epe, B.; Dall'Acqua, F.; Ramaiah, D.; Saha Möller, C. R. Photosensitized Formation of 8–Hydroxy–2'–deoxyguanosine in Salmon Testes DNA by Furocoumarin Hydroperoxides: A Novel, Intercalating Photo–Fenton Reagent for Oxidative DNA Damage. *Angew. Chem., Int. Ed. Engl.* **1995**, 34, 107–110.

(50) Arun, K.T.; Jayaram, D. T.; Avirah, R. R.; Ramaiah, D. β-Cyclodextrin as a Photosensitizer Carrier: Effect on Photophysical Properties and Chemical Reactivity of Squaraine Dyes. *J. Phys. Chem. B*, **2011**, 115, 7122–7128.

Table of Contents Graphics

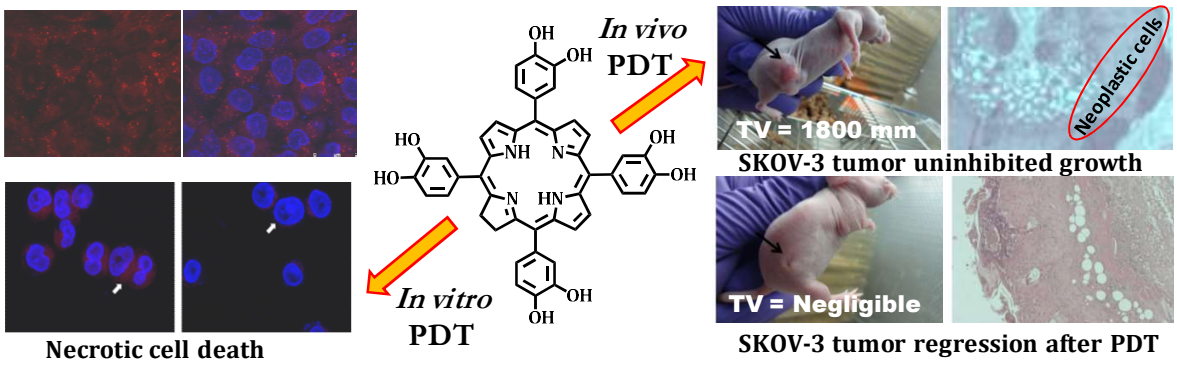

Table of Contents Graphics